Available online at www.sciencedirect.com
ScienceDirect
Scripta Materialia 58 (2008) 663–666
Scripta MATERIALIA
www.elsevier.com/locate/scriptamat

Temperature rise in severe plastic deformation of titanium at small strain-rates

C. Huang,[a] T.G. Murthy,[a] M.R. Shankar,[b] R. M'Saoubi[c] and S. Chandrasekar[a,*]

[a] *Center for Materials Processing and Tribology, School of Industrial Engineering, Purdue University, West Lafayette, IN 47907-2023, USA*
[b] *Department of Industrial Engineering, University of Pittsburgh, Pittsburgh, PA 15261, USA*
[c] *Seco Tools AB, SE-73782 Fagersta, Sweden*

Received 17 October 2007; revised 25 November 2007; accepted 29 November 2007
Available online 31 December 2007

Temperature rise in severe plastic deformation (SPD) of titanium at small strain-rates by machining has been measured using infrared thermography. The temperature rise is shown to be small and unlikely to influence material behavior during the deformation. The temperature distribution in the deformation zones is similar to the strain-rate distribution therein. The deformation mechanisms operative during the SPD are interpreted in terms of the observed temperatures and strain-rates.

Keywords: Severe plastic deformation (SPD); Machining; Titanium; Temperature

Due to its inherent simplicity, severe plastic deformation (SPD) has emerged as an attractive approach for the creation of bulk metals and alloys with ultrafine-grained (UFG) microstructure and enhanced strength and hardness [1–5]. In moderate-to-high strength materials with limited ductility (e.g. titanium, Al-6061T6), conventional SPD techniques such as equal channel angular pressing (ECAP) can only be performed at elevated temperatures, where the flow characteristics of the material (e.g. increased ductility, reduction in yield strength) facilitate large strain deformation. For example, UFG titanium, which is of particular interest for high-temperature structural applications, has been produced by deforming Ti to large strain values by using ECAP at temperatures of ~400 °C [1,2]. In some of these studies, the microstructure refinement was found to be insufficient to produce the desired properties and an additional deformation process, such as cold rolling, was used to further refine the microstructure [2].

Recently, large-strain machining has been shown to be an effective way of achieving SPD without preheating of samples, even for materials of high strength and limited ductility [5,6]. In Ti, the material that received the highest levels of strain, the chip, was found to have a nanocrystalline structure with ~100 nm size grains. This microstructure was finer than that observed in Ti following ECAP at elevated temperatures. However, questions pertaining to the magnitude of the temperature in the deformation zone and time duration for which the material experiences this temperature during the SPD were not directly resolved in these prior studies. Here, we report on the in situ measurement of the temperature distribution in Ti during SPD and show that under conditions of small strain-rates, the deformation indeed occurs at near-ambient temperature. The implications of this observation for microstructure development in hexagonal close-packed (hcp) material systems, in which only a limited number of slip systems operate at near-ambient temperature, and for machining as a method of SPD, are discussed.

Commercially pure Ti was deformed to large strains without preheating of the sample in a specially devised large-strain machining setup (Fig. 1). The bulk Ti sample, in the form of a plate, had an initial grain size of ~60 μm and a Vickers hardness of 144 kg mm^{-2} (300 g load). Characterization of the bulk material using X-ray diffraction confirmed the presence of only the hcp phase and an absence of any retained body-centered cubic (bcc) Ti. The machining conditions were similar to those used in earlier studies of SPD of Ti [6,7]. A high-speed steel tool of rake angle +20° was used to create chips in the form of foils with a width of 3 mm. An undeformed chip thickness (a_0) of ~300 μm and a

* Corresponding author. E-mail: chandy@ecn.purdue.edu

1359-6462/$ - see front matter © 2007 Acta Materialia Inc. Published by Elsevier Ltd. All rights reserved.
doi:10.1016/j.scriptamat.2007.11.042

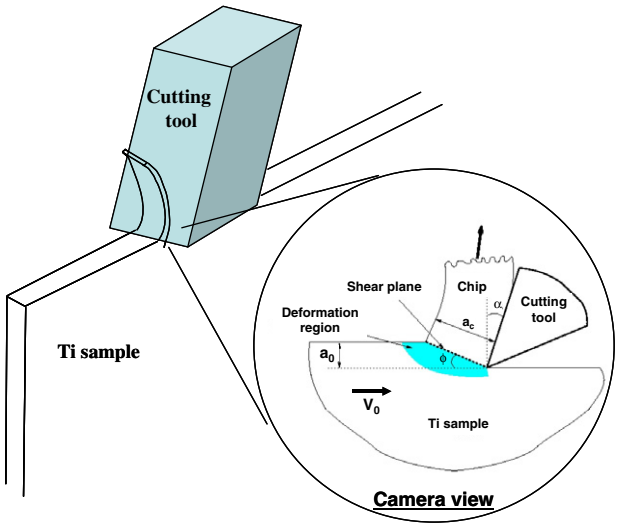

Figure 1. Schematic of plane-strain machining configuration used for SPD of Ti. A side of the sample shown in the inset is observed and imaged using a high-speed imaging system with PIV, and a CCD-based IR imaging system, to estimate deformation field parameters and temperature distribution, respectively.

cutting speed of 10 mm s^{-1} were employed to realize the large strain deformation. The Ti chip foil consisted of ~100 nm subgrains with a Vickers hardness of 230 kg mm^{-2} [6,7]. Direct observational techniques utilizing particle image velocimetry (PIV) [8] and infrared (IR) thermography [9] were used to measure the deformation and temperature fields, respectively.

Figure 1 shows a schematic of the experimental arrangement used to observe the deformation. One side of the Ti plate sample was constrained by a transparent glass block to ensure minimal side flow of the material during the chip formation while enabling direct observation of material flow through the deformation zones. In the first series of experiments, a sequence of images, in time steps (Δt) corresponding to the framing rate of a high-speed charge-coupled device (CCD) camera (Kodak Motion Coder Analyzer Sr-Ultra), was collected to characterize the deformation field parameters, i.e. velocity, strain-rate and strain. By following the motion of "asperities" specifically introduced onto the side face of the sample and applying an adaptation of a PIV technique, an image correlation method, the velocity, strain-rate and strain fields in the deformation zones were obtained [6,8].

In a second series of experiments under the same SPD condition, the temperature distribution in the deformation zones was measured using a CCD-based IR imaging system [9]. For this purpose, one side of the sample was coated with a "black" paint (Rutland Stove Paint) of high emissivity ($\varepsilon \approx 0.92$). A medium wavelength, high-speed IR imaging system (Galileo, Amber-Raytheon) was used to measure the radiation emitted from the deformation zone (Fig. 1), this radiation intensity being converted to temperature values using results from a calibration experiment. The imaging system consists of a CCD detector array and an IR microscope assembly. The microscope assembly focuses the IR radiation onto a two-dimensional focal plane array (FPA) of 256 × 256 detectors, effectively creating an image of the source on the FPA. The FPA is a two-dimensional CCD array of indium antimonide (InSb) detector elements (pixels) that are highly sensitive to radiation in the medium-wavelength IR range. With the 3X objective lens used in the present study, the size of each of the pixels is 10 μm × 10 μm and the field of view is 2.56 mm × 2.56 mm. The pixels of the FPA have a time constant low enough to enable system operation at shutter speeds as small as 2 μs, which allows for observation of transient events. A band-pass filter is fitted into the microscope assembly to cut off radiation outside a specific spectral range depending on the temperature range of interest. A value for the temperature at various locations in the deformation zones was obtained by averaging over 30 radiation intensity images acquired during the steady-state portion of the SPD. It is this averaged temperature value that is reported.

Radiation intensity values were converted to equivalent temperature values using a calibration experiment. This experiment involved focusing the IR imaging system onto a heated calibration sample, coated with the same black paint as that used on the Ti sample subjected to the SPD. A K-type thermocouple was attached to the calibration sample in the region from which the radiation intensities were recorded. As the sample was heated using a hot plate, intensity and temperature values were measured simultaneously by the imaging system and thermocouple, respectively. The calibration experiment was performed in the temperature range 30–250 °C. Further details of the temperature measurement procedure, including the calibration and correction for stray radiation, may be found elsewhere [9].

Figure 2 shows the variation in shear strain-rate determined using the PIV in the region ahead of the tool. Based on the strain-rate values, two distinct zones of deformation may be identified: a fan-shaped deformation zone well ahead of the tool wherein the strain-rate increases gradually, followed by a narrow zone of local-

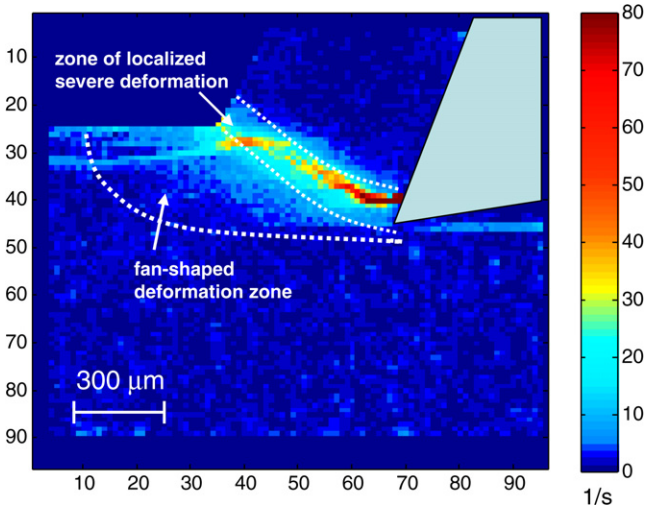

Figure 2. Distribution of shear strain-rate (strain-rate field) derived from the PIV showing two distinct deformation zones characterized by different intensities of strain-rate and strain-rate gradient. The units of strain-rate are per second.

ized severe deformation just ahead of the tool in which the shear strain-rates are much larger. The representative shear strain-rate in the zone of localized deformation is $\sim 40\ s^{-1}$ (for the machining speed of $10\ mm\ s^{-1}$), which is relatively small; hence, this SPD may be termed as "small" strain-rate deformation. The effective strain imposed in the chip material is ~1.5 as estimated by the PIV [6]. Other PIV measurements showed the strain-rate to vary linearly with machining velocity, especially at velocities of $1–50\ mm\ s^{-1}$. This observation suggests the possibility of varying the strain-rate over a wide range in this SPD, in contrast to ECAP and high-pressure torsion, since machining can be carried out at velocities of up to several meters per second. Previous work has shown a similarity between the morphologies of the deformation zones determined using the PIV (Fig. 2) and those observed metallographically, with a preponderance of twinning and elongated grain structures in the fan-shaped deformation zone and complete obliteration of metallographic features in the zone of localized deformation [6].

Figure 3 shows the temperature distribution in the deformation zones during the SPD, as derived from the IR radiation measurements. Three distinct zones of temperature are seen in this figure, two of which correspond to the deformation zones identified earlier in the shear strain-rate field. The fan-shaped deformation zone is characterized by a temperature of 80–100 °C with relatively gentle temperature gradients, while a representative temperature value of ~140 °C is characteristic of the zone of localized severe deformation together with much steeper gradients. The highest temperature value of ~160 °C occurs in a small zone located in the chip that partially overlaps with the zone of localized severe deformation. These temperature values are well below the softening temperature of Ti as well as small compared to 400 °C, the temperature to which bulk Ti has been preheated to in many prior ECAP studies [1,2]. Thus it is appropriate to consider this SPD of Ti as occurring at near-ambient temperature, a term used in prior descriptions of this small strain-rate deformation by machining [6,7]. It should be noted that no shear localization was observed in the deformation/temperature field or in the microstructure.

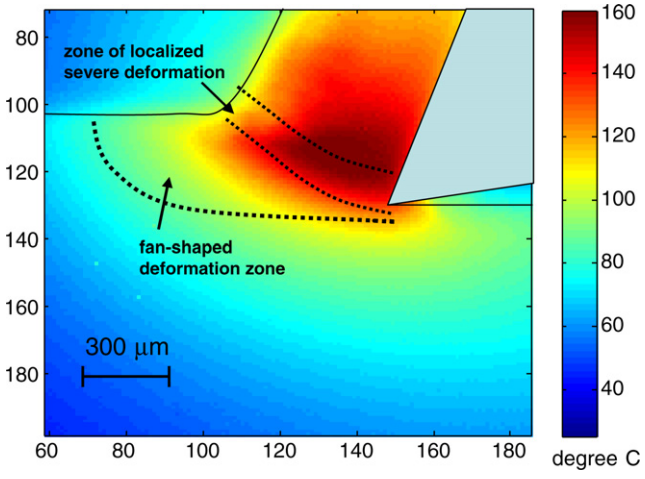

Figure 3. Distribution of temperature in the deformation zones. The deformation zones have been superimposed here from the shear strain-rate field (Fig. 2). Note the similarity between the temperature and strain-rate distributions.

While the temperature rises observed here are too small to impact material behavior, it is nevertheless of interest, in general, to consider the time for which the material is exposed to the "elevated temperature" during the SPD, in the context of understanding the role of thermal phenomena on the deformation. This may be done by estimating the time taken by any elemental volume of material to traverse the deformation zones and the zone of highest temperature in Figure 3. Assuming a value of $10\ mm\ s^{-1}$ for the velocity of material flow through the fan-shaped deformation zone (bulk material velocity), and a value of $4\ mm\ s^{-1}$ for the chip velocity (estimated by the PIV), it is easy to see that this time at elevated temperature is no greater than 100 ms for this SPD.

The observed similarity between the shear strain-rate (Fig. 2) and temperature fields (Fig. 3) is to be expected, for the temperature field is a direct consequence of the heat source distribution. The local heat source in any deformation process is directly proportional to the product of the shear yield strength and the strain-rate. Since the yield strength of the Ti is likely to be negligibly affected by temperature and strain-rate, given their relatively small values for this SPD condition, the heat source distribution is directly related to the strain-rate distribution. Hence, to first order, the temperature distribution (field) should be expected to mirror the strain-rate distribution (field), as has indeed been noted.

The temperature field also indicates that even at the small machining speed of $10\ mm\ s^{-1}$, the temperature rise is the greatest in the chip in a region that overlaps with the zone of localized severe deformation; this region is, however, located well away from the fan-shaped deformation zone. Furthermore, this region of highest temperature moved up into the chip and away from the zone of localized deformation when the machining speed was increased only slightly to a value of $50\ mm\ s^{-1}$ (strain-rate $\sim 200\ s^{-1}$). This is characteristic of moving heat sources associated with deformation, wherein the kinetics of heat transfer are modified by mass transport of material through the deformation zones [10]. That is, even though the heat is generated during the SPD mainly in the zone of localized severe deformation, the temperature rise is not merely dictated by the thermal diffusivity of the medium, but modulated by the mass transfer associated with the material that traverses the deformation zone, carrying with it the thermal energy into the chip material and away from the region of the SPD. This characteristic ensures that the deformation zone is at near-ambient temperature and, therefore, the mechanics of deformation are similar to those expected in Ti at room temperature. This aspect became apparent following electron back-scatter diffraction (EBSD) analysis of the twinning observed in the fan-shaped deformation zone [11]. Figure 4 shows these twins to be predominantly of the $\{1\bar{2}10\}$ system, which is identical to that observed during room temperature SPD in surface mechanical attrition treatment (SMAT) of Ti [12]. This observation further reinforces the case

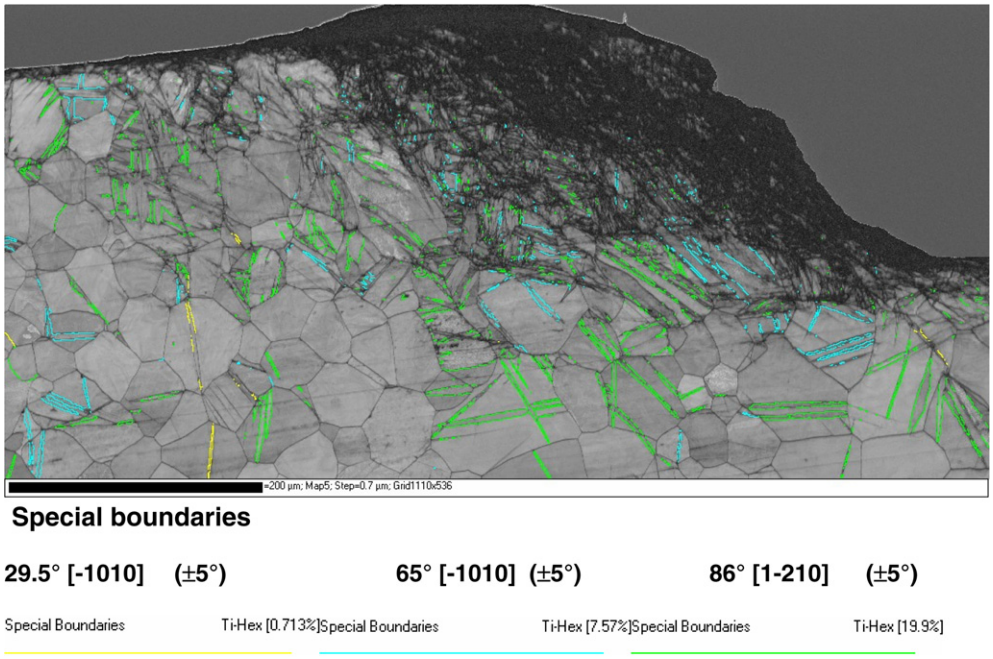

Figure 4. EBSD analysis of the fan-shaped deformation zone. The special boundaries corresponding to the twin structures are indexed to reveal a preponderance of the $\{1\bar{2}10\}$ system.

for chip formation in machining as an SPD process at near-ambient temperatures, even for difficult-to-deform materials such as Ti.

We would like to thank Ms. Lena Ryde (Corrosion and Metals Research Institute, Stockholm, Sweden) for helping with the EBSD study. We are grateful to the US Department of Energy (grant 4000031768 via UT-Battelle), the NSF (grant CMMI 0626047) and the State of Indiana 21st Century Research and Technology Fund for supporting this work.

[1] V.V. Stolyarov, Y.T. Zhu, T.C. Lowe, R.Z. Valiev, Journal of Nanoscience and Nanotechnology 1 (2001) 237.
[2] Y.T. Zhu, J.Y. Huang, J. Gubicza, T. Ungar, Y.M. Wang, E. Ma, R.Z. Valiev, Journal of Materials Research 18 (2003) 1908.
[3] I. Kim, J. Kim, D.H. Shin, X.Z. Liao, Y.T. Zhu, Scripta Materialia 48 (2003) 813.
[4] D.H. Shin, I. Kim, J. Kim, Y.S. Kim, S.L. Semiatin, Acta Materialia 51 (2003) 983.
[5] M.R. Shankar, S. Chandrasekar, A.H. King, W.D. Compton, Acta Materialia 53 (2005) 4781.
[6] M.R. Shankar, B.C. Rao, S. Lee, S. Chandrasekar, A.H. King, W.D. Compton, Acta Materialia 54 (2006) 3691.
[7] M.R. Shankar, R. Verma, B.C. Rao, S. Chandrasekar, W.D. Compton, A.H. King, K.P. Trumble, Metallurgical and Materials Transactions A 38 (2007) 1899.
[8] S. Lee, J. Hwang, M.R. Shankar, S. Chandrasekar, W.D. Compton, Metallurgical and Materials Transactions A 37 (2006) 1633.
[9] J. Hwang, S. Kompella, S. Chandrasekar, T.N. Farris, Journal of Tribology 125 (2003) 377.
[10] M.C. Shaw, Metal Cutting Principles, second ed., Oxford University Press, Oxford, 1984.
[11] R. M'Saoubi, L. Ryde, Materials Science and Engineering A 405 (2005) 339.
[12] K.Y. Zhu, A. Vassel, F. Brisset, K. Lu, J. Lu, Acta Materialia 52 (2004) 4101.